http://eprints.gla.ac.uk/121085/

Deposited on: 16 July 2016

Acoustic Comparison of Propellers

G.N. Barakos and C.S. Johnson

CFD Laboratory, School of Engineering
University of Glasgow, G12 8QQ, Scotland, United Kingdom

g.barakos@glasgow.ac.uk

Abstract

This paper presents results of Computational Fluid Dynamics (CFD)results for flows around propellers and compares their aerodynamic performance as well as their acoustics. After some validation of the employed CFD method, using wind tunnel experiments, a modern propeller design was assessed. Using the same baseline blade, different propellers were put together by adding stagger at the blade hub and small variations of the inter-blade angle. The employed method produced results showing differences in the propeller acoustics regarding the frequency spectrum produced by each design and the level of the acoustic tones. The effect of chancing the hub was to generate frequencies in-between the tones of the baseline design while keeping the overall propeller performance the same. The effect of the employed hub changes was to generate tones in-between the harmonics of the fundamental blade passing frequency that dominated the baseline design. Installed and un-installed blades were compared and the results show that the wing, nacelle and fuselage around the blades, influence the obtained level of noise but not the frequency content. Computations for a climbing case also show the strong effect of the flight conditions on the acoustic results.

Key Words: *Propeller noise, Computational Fluid Dynamics, Computational Acoustics*

1 INTRODUCTION

Research in propeller acoustics is fueled by the need for transport aircraft with low impact on airport and community noise and high propulsive efficiency. This combination of characteristics is difficult to achieve even with modern turbo-prop aircraft.

Previous work on propeller aerodynamics and acoustics includes the work by Jeracki and Mitchell [3] where the SR propeller series of NASA (National Aeronautics and Space Administration) was used to test advanced design concepts for high speed turbo-prop aircraft. Different number of blades, planform designs and conditions were tested and compared. Acoustic research is also presented by Woodward and Loeffler [13] and McCurdy [5] with emphasis on the in-flight noise and the annoyance caused on the ground by over-flying turbo-prop aircraft.

Interior fuselage noise was measured on a SAAB 2000 aircraft and reported by Samuelsson et al. in [4]. Differences in starboard and port noise were found and interference from other aircraft components were analysed.

A more recent work by Pechan and Sescu [8] looked at the effect of small manufacturing imperfections on the acoustics of propellers. Experiments were conducted but were limited to small-size propellers suitable for unmanned aerial vehicles (UAV). Their work is representative of several other studies motivated by the recent trend in the use of small UAVs. Wang *et al.* [12] employed advanced Large-Eddy Simulation methods combined with Finite Elements to look at propeller noise but their work considered marine propellers. Likewise, the work of Wu and Li [14] also employed advanced fluid/structure interaction methods for acoustics studies of marine propellers. This is a trend clearly seen in the current literature with the most advanced CFD methods employed for the analysis of marine propellers while less work is reported related to the use of advanced simulation tools for high-speed, transonic aircraft propellers. One exception is the work of Muller *et al.* [7] that concerns the performance of a propeller-wing configuration at high Mach number.

The above observations set the objectives of this paper that attempts to use Computational Fluid Dynamics as a tool for comparing the acoustics of different propeller designs for large turbo-prop aircraft, revealing differences in noise as a result of modifying the arrangement of the blades on the propeller hub. The effect of having the propeller installed on an aircraft is also investigated and contrasted with results for isolated propeller acoustics. This work is part of the IMPACTA (Improving the Propulsion Aerodynamics of Turboprop Aircraft) project of GE-DOWTY (General Electric - Dowty Propellers) that provided the baseline blade design. Starting from a given blade shape, different hub arrangements are compared with CFD in terms of their acoustics. The overall strategy followed in this work, is to introduce slight changes to the hub and planform of the propeller so that the frequency content of the propeller as well as the peaks of its tones are modified.

2 GEOMETRY AND CONDITIONS FOR COMPUTATIONS

The IMPACTA propeller was designed for high efficiency at high speeds due to its swept back blades, the large number of blades and the thinner aerofoil sections employed. Its larger diameter allows for less power loading even though more thrust is obtained. This improves the efficiency as it reduces the amount of swirl in the wake due to engine torque.

The baseline design was an 8-bladed propeller of aspect ratio 10.4 and root chord length of 0.213 metres. It was modified by introducing staggering of the blades near the hub or by changing the inter-blade angles in a symmetric way. Moving four out of the eight blades slightly forward is expected to change the acoustic signature of the blades and provides a different distribution of the emitted acoustic energy between frequencies. The same effect is expected by changing the inter-blade angle between

every other blade of the propeller. The blades were designed to run at 856 Revolutions Per Minute (RPM). Figure 1 presents the different hub arrangements for the baseline, stagerred and unequally-spaced configurations, as compared in this work.

An offloaded tip variation of the baseline blade was also analysed. The offloaded blade has about 1.8º less twist than the baseline blade and approximately 2 degrees more pitch at 70%R. It was also run at 790 RPM . Figure 2 shows the twist difference between the baseline and offloaded blade designs.
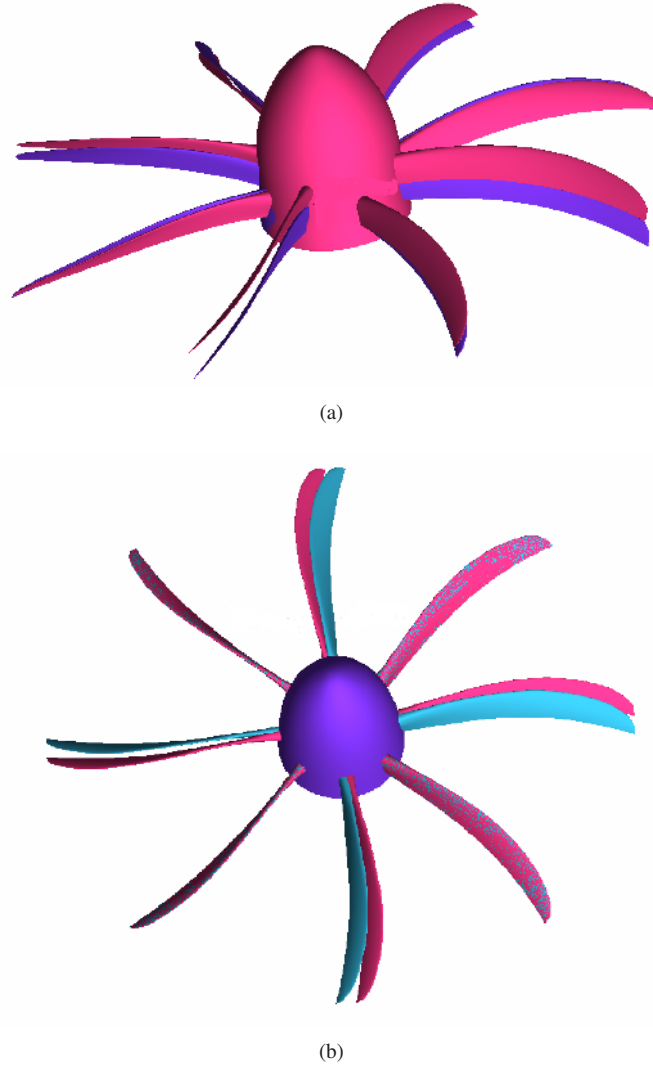
(a)

(b)

Figure 1: Comparison of (a) Baseline and Staggered, and (b) Baseline and Unequally-spaced propeller designs.

2.1 Conditions for Computations

Several flight conditions were selected and the ones used for comparisons are summarised in Table 1. The nominal rotation speed was $\Omega = 89.7$ rad/s. The propeller thrust coefficient is given by the following equation:

$$C_T = \frac{T}{\rho \omega^2 D^4} \tag{1}$$

where D is the diameter of the propeller. To trim the propellers to a required thrust, small adjustments of the blade pitch were possible by deforming the CFD mesh. For the work presented here the necessary changes were of the order of 0.25 degrees. The conditions at altitude were found using the ideal gas equations and the international standard atmosphere. The Reynolds number was found to be approximately 1 million based on the root chord of the blade and the tip Mach number was 0.627. The two flight conditions selected for computations were named "cruise" and "climb" and are summarized in Table 1 below.
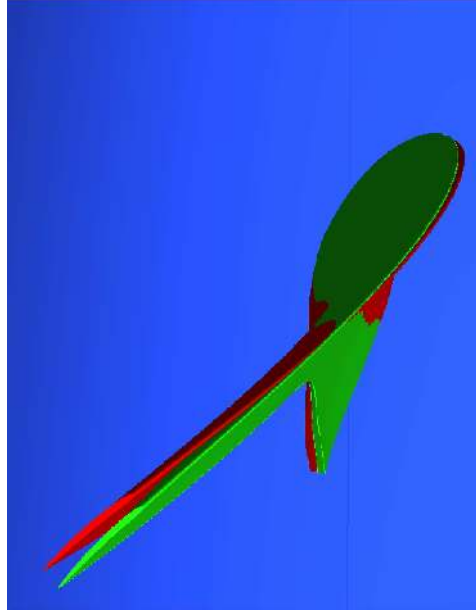
(a)

Figure 2: Comparison of Baseline and Offloaded blade designs.

	CRUISE	CLIMB
Altitude (m)	7620	6096
Temperature (ISA + °C)	10	10
Cruise Mach Number	0.5	0.44
Required thrust (N)	7851	12722
Tip speed (m/s)	198	198
RPM	856	856
Pressure at altitude (Pa)	37581	46544
Density at altitude (kg/m^3)	0.527	0.627
Temperature at altitude (K)	248.6	258.5
Speed of sound (m/s)	316	322

Table 1: *Cruise and climb flight conditions employed for computation.*

3 CFD METHOD

CFD is used as the primary tool for analysing the acoustics of the propellers, and all calculations were performed using the Helicopter Multi-Block Method (HMB2) taking advantage of its ability to perform steady-state periodic or fully unsteady computations [2] using the RANS (Reynolds-Averaged Navier-Stokes) and URANS (Unsteady Reynolds-Averaged Navier-Stokes) approach or even Scale-Adapted Simulation (SAS) [6] and Detached-Eddy Simulation (DES) [10]. For this work, fine multi-block grids were used with the sliding plane method [11] to account for the relative motion between the airframe and the propeller. The propeller grids had approximately 12 million cells per blade for the isolated cases. It was assumed that the propeller blades are rigid. The grid size for the installed cases was increased to 50 million cells. To compute the isolated propeller cases 12 hours of CPU time on 128 Intel Xeon cores operating at 3.40GHz were adequate. For the installed cases, the time was increased to 22 hours per revolution and four revolutions were the minimum for the flow to be resolved.

For the cases presented in this paper, the Reynolds Averaged Navier-Stokes (RANS) method was used with the $\kappa - \omega$ turbulence model to obtain CFD results and analyse the predicted acoustic tones. No far-field acoustics method was used since only the near-field tonal noise is of interest in this work. This noise is well-resolved within the framework of the URANS equations, provide a good numerical scheme and a fine mesh are used. HMB solves the Navier Stokes (NS) equations in integral form and discretises them using a cell-centred finite volume approach on structured multi-block grids. Temporal integration is performed using an implicit dual-time stepping method. The details of the theory behind this method and its derivation can be found in the work of Anderson [1].

The acoustic analysis is carried out by comparing the sound pressure level (SPL) at specified locations termed "probes".

3

These SPLs are obtained using the unsteady pressure obtained from the CFD solution. The primary objective of the acoustic analysis is to determine the noise heard by passengers in an aircraft. Therefore, the time and space resolution required must be such that the frequencies detected are within the audible range (20 - 10000 Hz). Using Nyquist's theorem, to capture 10 kHz, means that the sampling frequency required is 20 kHz. Therefore the largest time step required is 5×10^{-5} seconds. Since the rotation rate of the propeller is 856 RPM, this means that an azimuth of 1 degree takes approximately 1.94×10^{-4} seconds. Therefore a time resolution of about a quarter degree is required to capture the audible frequencies.

For the spacial or grid resolution, a frequency of up to 4000 Hz should be able to be resolved directly as tonal noise. Higher frequencies are expected to be due to broadband noise. If a frequency of 4000 Hz at the cruise conditions is to be obtained, the wavelength to be resolved can be found as:

$$\lambda = v/f = 0.08m \tag{2}$$

Using the speed of sound at the selected conditions (316 m/s), if 10 points are used to describe the shape of the wave, then a grid resolution of 0.008 metres is required. Therefore the non-dimensional resolution of the grid can be calculated using the reference length, which in this case is the root chord of the blade as 0.0371 c. The nearest probe on the fuselage was 1 metre away from the blade. Therefore, at least 126 cells were needed between the blade and the fuselage. In the mesh used for the computations, there were 112 cells distributed normal to the blade surface, such that the boundary later is also captured.

4 CFD VALIDATION USING THE JORP PROPELLER

The Joint Open Rotor Propeller (JORP) model blade was used for comparisons with experiments. It consisted of a single row of six blades mounted on a spinner designed for minimum interference [9]. The blade sections used were high speed designs from a family of aerofoils designed by the Aircraft Research Association and Dowty Propellers, and were incorporated at 0.6 and 0.95 r/R. A parallel nacelle was included at 0 pitch and yaw. The diameter was 0.914m (3ft) to create a higher disc loading. To measure the surface pressure, 28 pressure tapings were incorporated at each of the 9 radial stations between 0.35 and 0.95 r/R [9]. Typical cruise speeds were at Mach 0.65 for the un-swept blade. The tip speed was 180m/s. Figure 3 shows the geometry of the un-swept version of the JORP. Since the propeller was 6-bladed and the simulation can be assumed to be periodic, only one blade was meshed using periodic boundary conditions on the planes between blades. For one blade, the mesh contained approximately 12 million cells. The far-field was placed approximately 5 propeller radii away from the blade [11]. The hub was modelled as a cylinder for faster convergence of the steady-state simulation.

Figure 4 shows the surface C_p distribution in comparison to the experimental data at a number of radial locations along the blade. The C_p is obtained from the surface pressure distribution. The results agree fairly well with the experiments, even if no attempt was made to perfectly match the thrust of the propeller that was measured during experiments by altering the pitch angle of the blade during CFD computations.
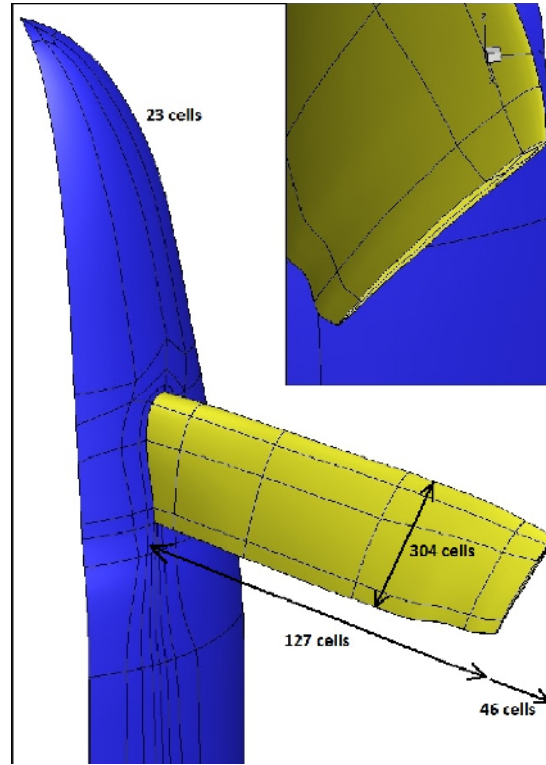
Figure 3: Grid geometry for the un-swept version of the JORP blade.

5 CFD RESULTS FOR THE IMPACTA BLADE

The topology used for the propeller grids is the same as that of the JORP mesh, and each blade was meshed using 12 million cells. Figure 5 shows the propeller installed on the port side of the aircraft.

For the installed cases, the block and mesh data for each component are given in Table 2. Each of these components was separated by a sliding plane. The size of the mesh is relatively large and this was shaped by two factors. First of all, the mesh was as fine or finer on the blades as for the JORP case. This ensured correct loads in terms of surface pressure. In addition, the spacing of the mesh away from the blade, and between the blades and the wing had to be fine enough to resolve at least 5-10 points for the wavelength of the 3rd harmonic of the blade passing frequency. Some of these sliding planes are shown in Figure 5. Overall, the sliding grids were used for two purposes. First, for isolating the rotating blades and spinner from the nacelle. This required 3 sliding planes on the drum surfaces of Figure 5. Secondly, sliding planes were used to isolate the multi-block topology used around he nacelle from the wing root and tip.

Grid Component	No. of Blocks	No. of Cells
Fuselage	208	4,566,404
Nacelle	1556	11,399,377
Wing	118	2,368,258
Baseline Propeller	3664	22,515,696
Staggered Propeller	2704	31,224,832
Unequal Propeller	2704	31,224,832

Table 2: *CFD grid components and their sizes.*

5.1 Isolated Propeller Aerodynamics

Figure 6 shows the surface pressure coefficient C_p at a station along the radius of the isolated baseline blade with the Baseline, Staggered and Unequal hubs. There are very small changes of the blade loading due to the changes in the hub. This also facilitates a fair comparison between the obtained acoustic spectra. Figure 7 compares the C_p of the two different blades i.e. the baseline, and offloaded designs with the baseline hub. The offloaded blade is pitched higher and hence has more loading inboards. The method used for the CFD computations employed a periodic domain and steady-state RANS simulations. Figure 8 shows the
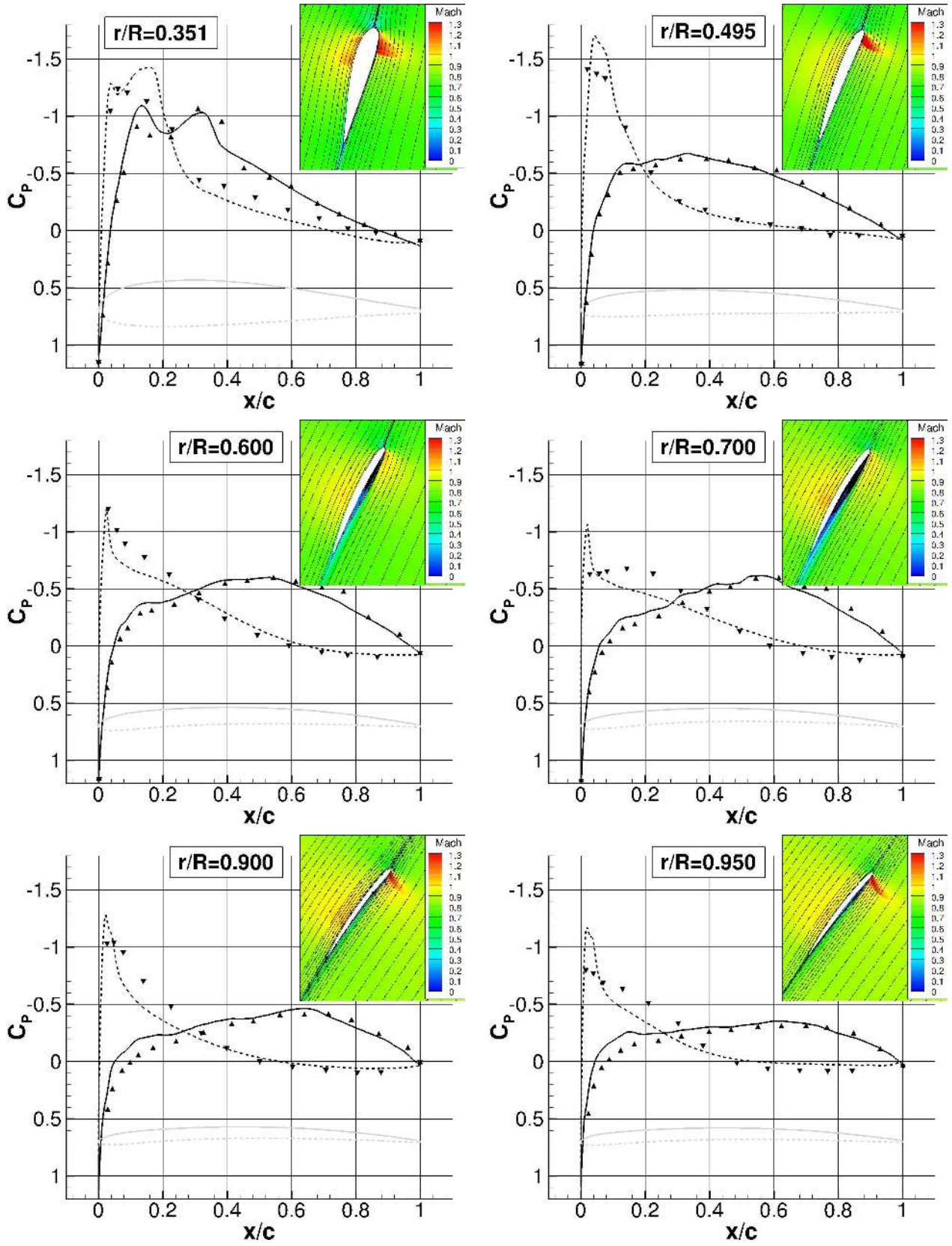
5

Figure 4: Surface pressure coefficient, C_p, distribution at a number of sections along the blade where experimental comparison can be made. The Mach number field is shown in the insert figures.

normal and axial force coefficient distributions along the blades. The distributions suggest that for most of the blade radius the employed hub modifications are not affecting the blade loads, at least outboards of the 45%R stations.
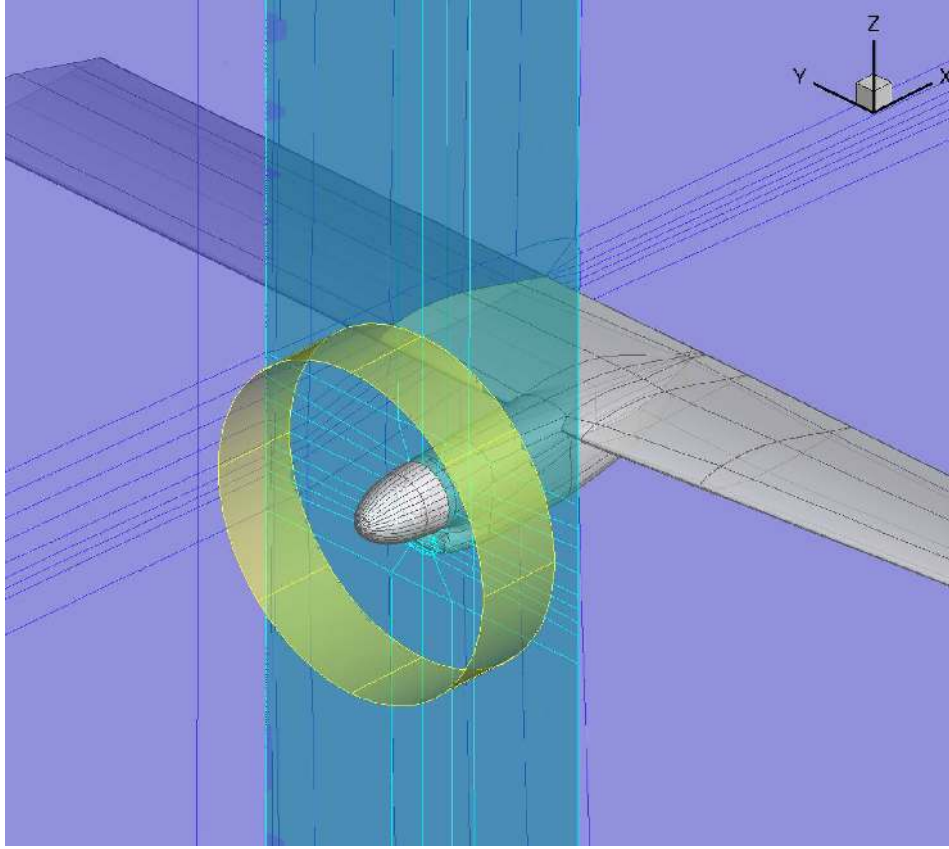
(a)

Figure 5: Multi-block topology, and sliding planes between the propeller and wing used for the installed case computations.
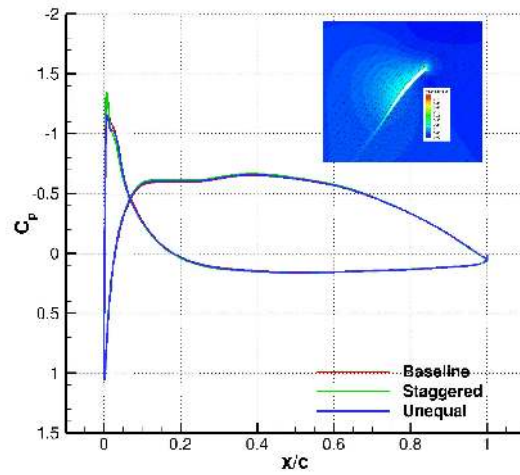
(a)

Figure 6: Surface pressure coefficient, C_p, for the Baseline, Staggered and Unequal hub with the baseline blade at r/R = 0.7. Cruise conditions, free-stream Mach = 0.5, tip Mach = 0.627, RANS calculations.

5.2 *Isolated Propeller Acoustics*

Figure 9 shows the probe positions where acoustic data is extracted from the CFD solution. The probes are on a fuselage that is at least 1 metre away from the tip of the blade. In this case, the results shown are for the propeller on the port side of the aircraft. Probe 776 is in the middle of the fuselage and in-line with the blade hub. Probes 760 and 792 are on the same line but on top
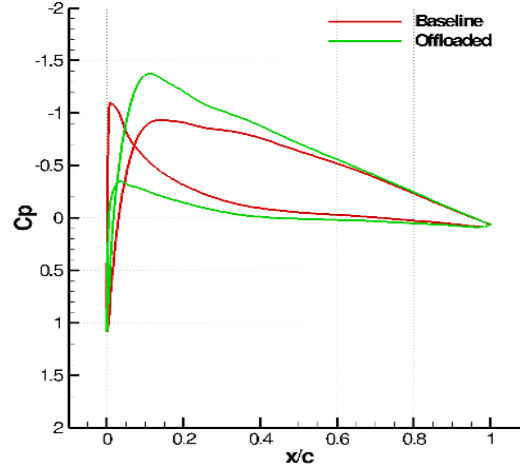
(a)
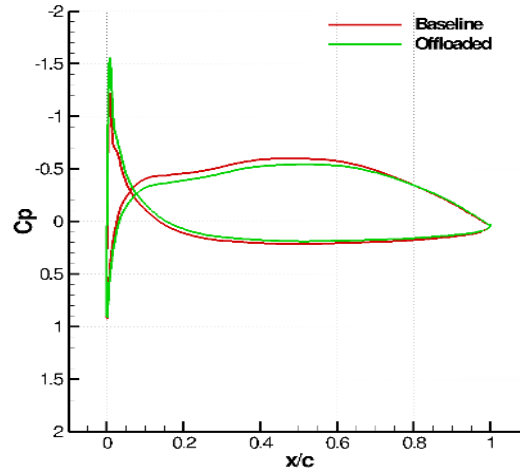
(b)

Figure 7: Surface pressure coefficient, C_p, comparisons for the baseline, and offloaded blades at three sections: (a) r/R = 0.5, and (b) r/R = 0.9. Cruise conditions, as given in Table1. Note that for the offloaded blade the tip Mach number was 0.579.

and below the fuselage. Although computations were performed in isolation without any nacelle or fuselage, the CFD was able to show the differences between the designs. An example of the spectrum is shown in Figure 10. The peaks from such a curve at the blade passing frequency are plotted in Figure 11 that shows the sound pressure level (SPL) spectrum for each of these probes with the different variations of hubs and blades. The figures show the maximum amplitude at the blade passing frequencies. It is clear that for the staggered and unequally spaced hubs, additional peaks occur at 4 per rev frequencies. This is because for these cases, there is a 4-per-rev periodicity either due to blade axial or azimuthal position. The relatively stronger noise of the peaks of the staggered design could be attributed to the presence of some blade-to-blade interference between the front and back blade-rows. Even though, having these additional peaks slightly increases the overall energy of the sound, the additional frequencies makes the periodicity of the signal less detectable and this changes the quality of the noise. In all three probes in line with the propeller plane, the baseline noise diminishes relatively quickly at higher frequencies. The offloaded tip generally has a slightly lower noise profile as well as a different Blade Passing Frequency (BPF) due to its lower RPM conditions. The approximate pitch angle at the 70% radial station in degrees is 50.1 for the Baseline, and 53.6 for the Offloaded blade.

A comparison is also made between unsteady and steady simulations as well as between two unsteady methods: URANS and the Scale Adaptive Simulation (SAS) developed by Menter [6]. Figure 12 shows this comparison for probe 776. Here, the unsteady pressure was estimated by removing the root mean square (rms) pressure over one period. It can be seen that the tonal noise has about the same amplitude but the broadband noise is slightly higher for the unsteady calculations. On the other hand, the unsteady computation did not show any change at the predicted tones.
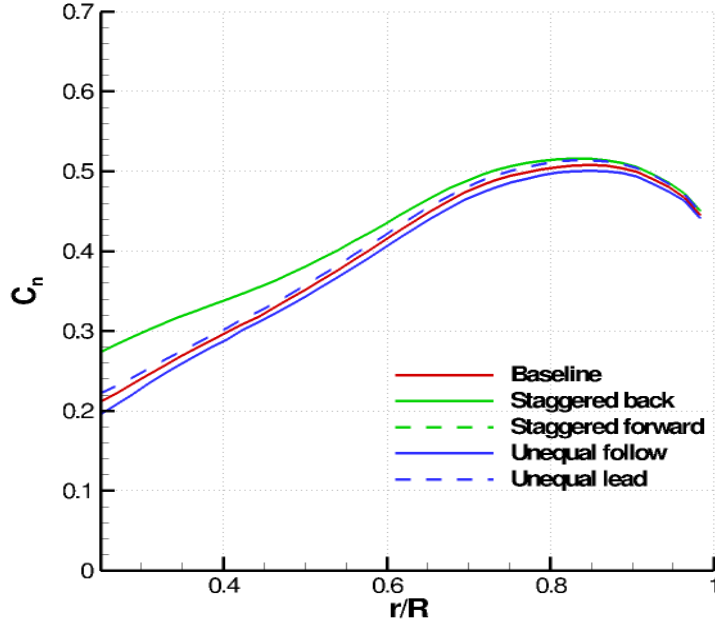
(a)
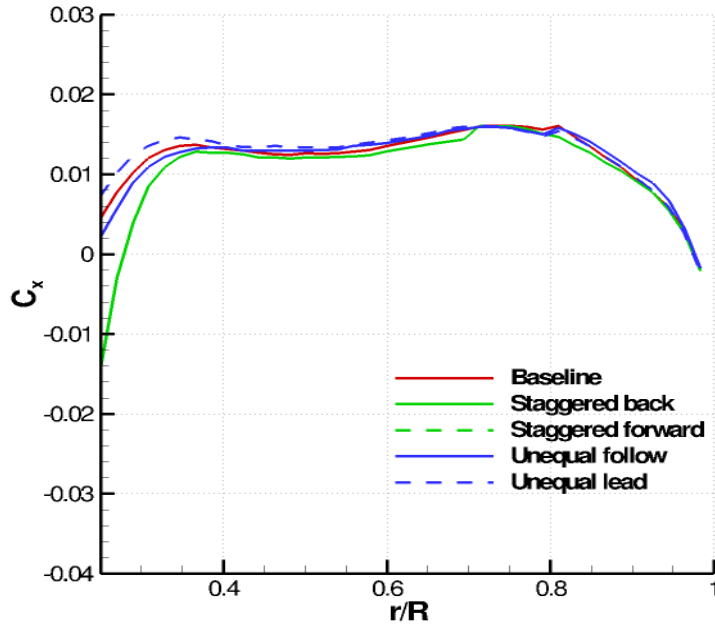
(b)

Figure 8: Normal and axial force coefficient distributions for the isolated blades at cruise conditions, free-stream Mach = 0.5, tip Mach = 0.627, RANS calculations.

5.3 Installed Propellers

Further results were obtained for installed configurations of the propellers using a half-model of a generic turbo-prop aircraft (designed as part of the IMPACTA project) and the same blades and hubs. An example of the surface C_p on the wing, nacelle, and fuselage is shown in Figure 13. The comparison shows the differences between cruise and climb flight conditions. Figure 15 compares the C_p distributions of the isolated and installed propellers. The installed blade is at 0 degrees azimuth i.e. vertically

9
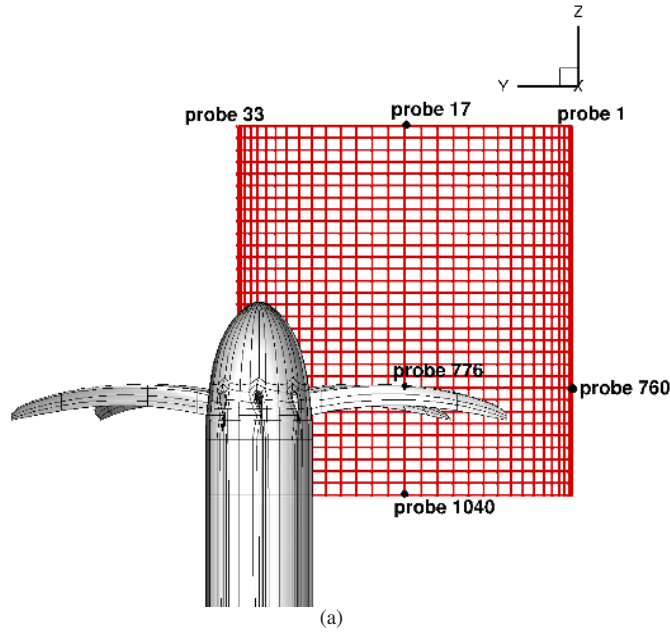
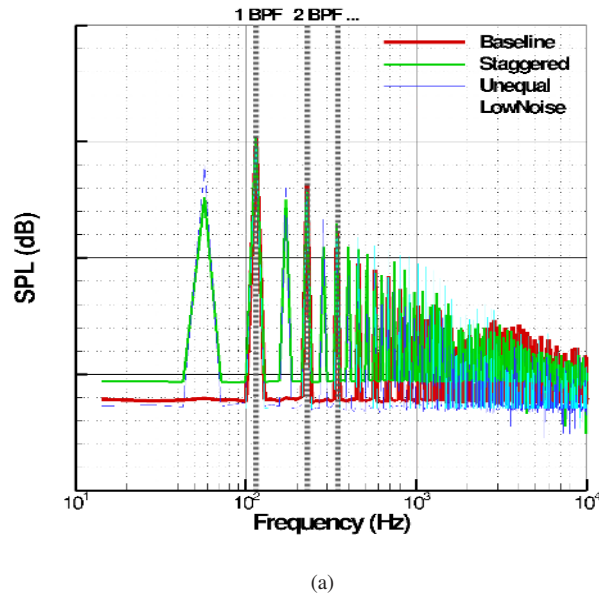Figure 9: Probe positions for monitoring the propeller acoustics.

Figure 10: SPL vs. Frequency(Hz) for the various configurations with the baseline blade at probe 776. Cruise conditions, free-stream Mach = 0.5, tip Mach = 0.627, RANS calculations.

upwards and has a significant drop in load due to the added aircraft components. This impacts the noise produced. Figure 14 shows the effect of the propellers on the wing loading of the aircraft, in particular, the lift distribution. It is given as a ratio of the loading to the baseline loading, hence a value of one for the baseline case itself. All the solutions are presented for the same blade azimuth. For the staggered blade, the differences in loading may be due to the fact that it also has a smaller hub and one set of the blades is closer to the wing. The offloaded blade is pitched higher, but its pitch distribution is different from the baseline blade between the root and tip. This is the reason for the differences in the variation of the load along the blade. Figure 16 shows the locations of all the probes for the installed cases. Figure 17 shows the frequency spectrum at one of these probes, probe 776 which is on the same plane as the propeller. It compares the spectrum for the installed and isolated propeller. There is quite a big difference in the broadband noise. However, the key comparison is in the peaks of the harmonics. In this case, the installed case has a louder SPL at the 1st blade passing frequency (BPF) and then drops off faster than the isolated.
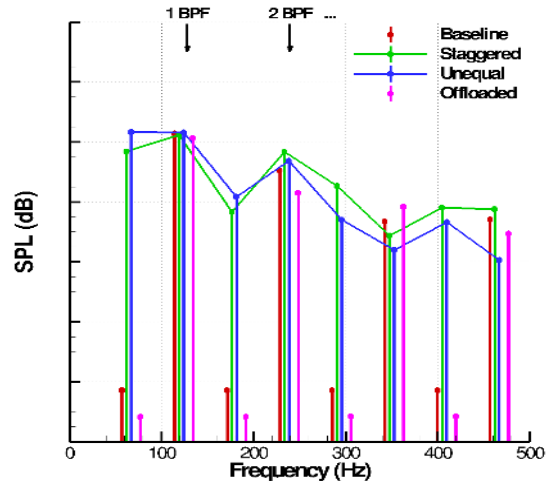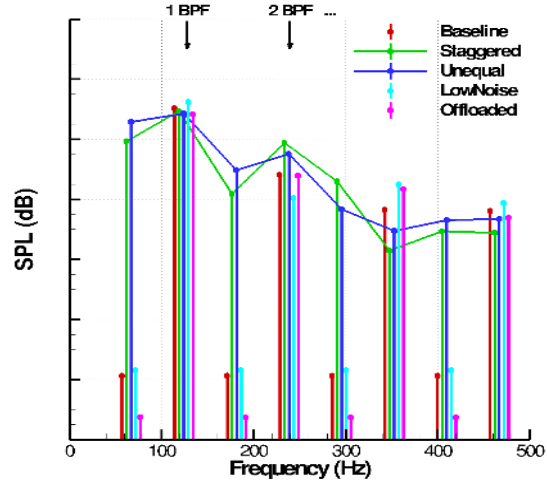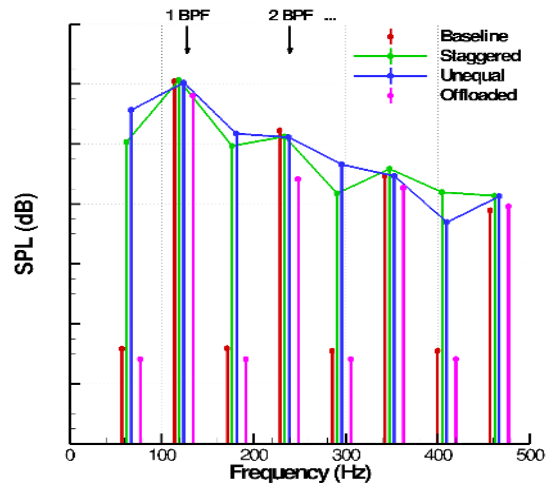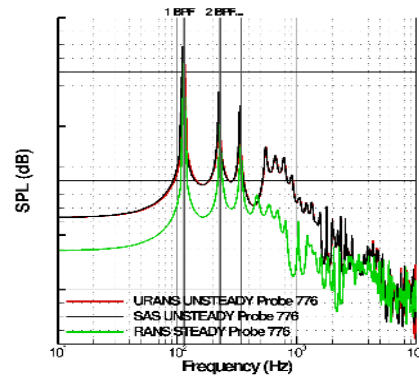
Figure 11: SPL at the Blade Passing Frequencies (BPF)(Hz) for the Baseline, Unequal and Staggered blades at three probe locations: (a) probe 760, (b) probe 792 and (c) probe 776. Cruise conditions, free-stream Mach = 0.5, tip Mach = 0.627, RANS calculations.
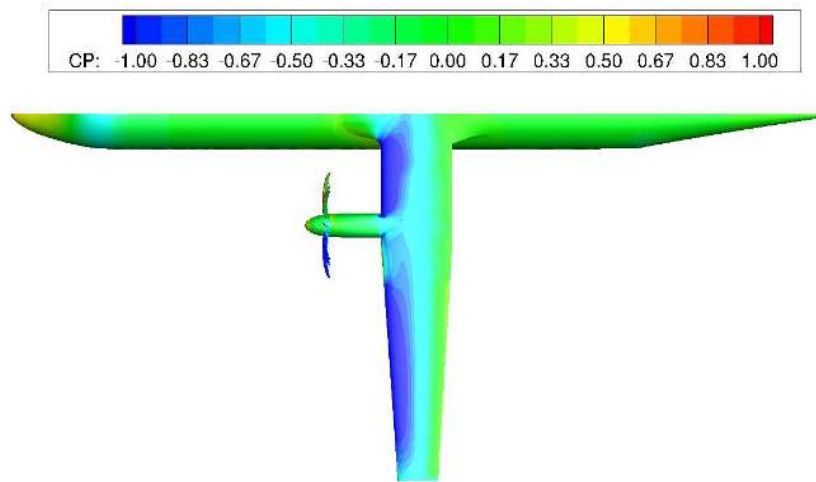
(a)

Figure 12: SPL vs. Frequency (Hz) for the Baseline at probe 776, cruise conditions, free-stream Mach = 0.5, tip Mach = 0.627 comparing SAS, URANS and RANS methods.
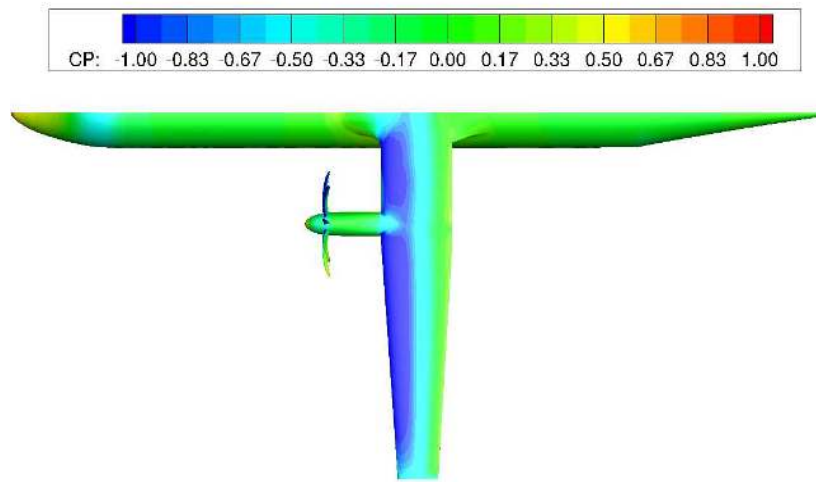
(a)

(b)

Figure 13: Surface C_p for the installed baseline propeller. (a) Cruise conditions (b) Climb conditions as per Table 1.
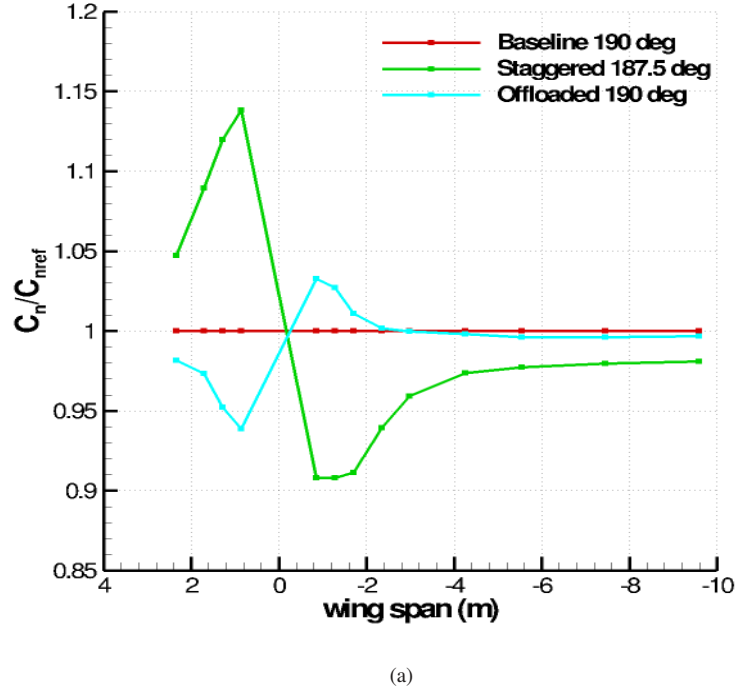
(a)

Figure 14: Comparison of the wing loading of the installed case with different propellers. For all cases the first blade is vertically upwards at 180 degrees azimuth. The computations correspond to cruise conditions, free-stream Mach=0.5, tip Mach=0.627. The blade loading of the baseline design is used as reference.
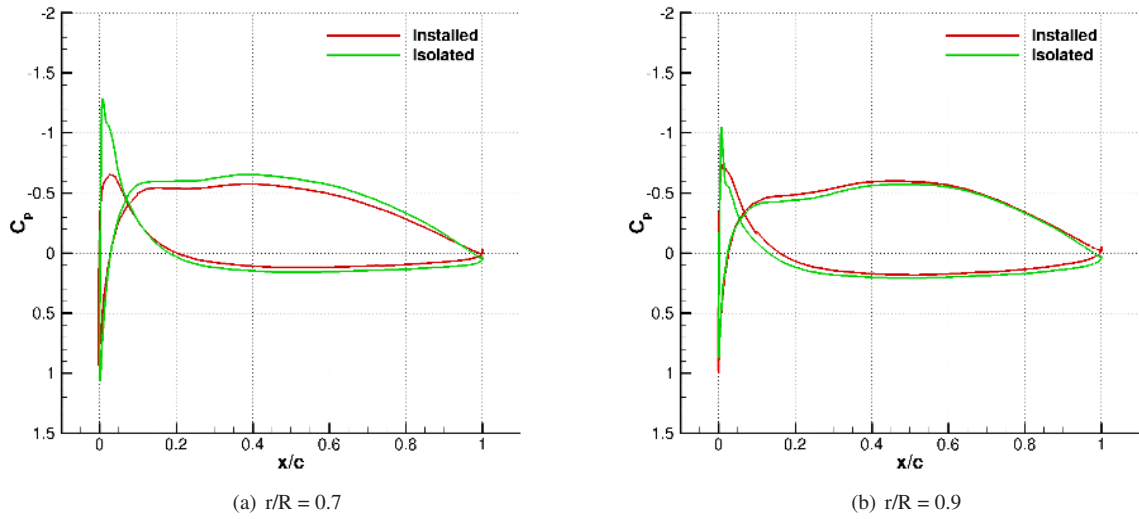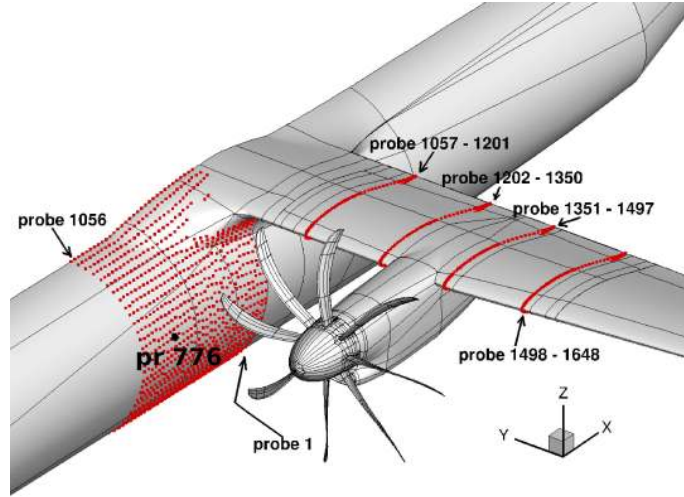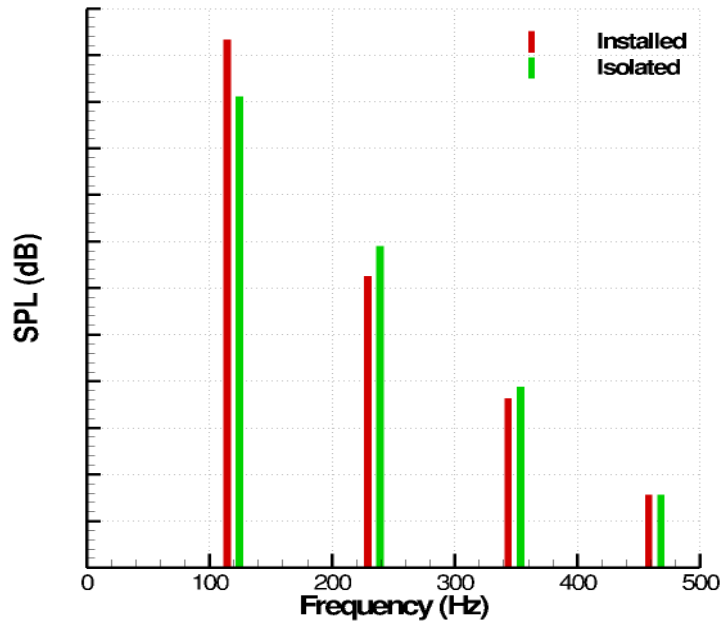

(a) r/R = 0.7

(b) r/R = 0.9

Figure 15: C_p on the blade at 0 degrees azimuth where blade is vertically upwards at cruise conditions in comparison with Isolated blade for the Baseline case.

(a)

Figure 16: Probe locations for the installed cases.

(a)

Figure 17: SPL vs. Frequency for probe 776 (middle of the fuselage in line with the propeller plane) with the isolated and installed cases. Cruise conditions, free-stream Mach = 0.5, tip Mach = 0.627.

6 CONCLUSIONS AND FUTURE WORK

The paper employed CFD to resolve the tonal acoustic content of the flow-field in the vicinity of modern propeller designs. The computations were mainly unsteady and the employed grids managed to resolve the details of the flow around different blade configurations. The paper presented the differences in the tonal acoustics of the assessed propeller designs and discussed the

effect of the different hub arrangements in terms of the acoustic tones and their magnitude. It also showed some of the differences between isolated and installed propeller noise. The isolated blade calculations predicted a change in the frequency content due to modifications of the hub. On the other hand, the level of the tones was not substantially reduced. The modifications break the strong tonal content of the baseline design and introduce additional frequencies that may lead to more acceptable noise characteristics by aircraft passengers. This change in the sound qualities introduced by staggering or off-setting the blades is seen not to have any substantial performance penalties. The proposed changes are also small and for this reason they may be easy to accommodate as part of the design of a new propeller hub without substantial penalties in its complexity and weight. The installed case showed an increase in the strength of the first harmonic and slightly faster drop at higher frequencies in comparison to the isolated propeller computations. The wing and propeller were computed at the same time and their interaction was resolved. The results also indicated differences in the loading of the propeller due to the presence of the wing, as well as, a strong effect of the propeller wake on the downstream part of the wing. This result suggests that comparisons between installed blades are required if firm conclusions are to be drawn on the advantages of any of the proposed blade configurations.

Further work is therefore to be carried out with installed cases, and this includes comparison with experiments envisaged in the near future.

REFERENCES

[1] J. D. Anderson, Jr. *Computational Fluid Dynamics, The Basics with Applications*. McGraw-Hill International Editions, 1995.

[2] A. Brocklehurst, R. Steijl, and G.N. Barakos. CFD for tail rotor design and evaluation. In *34th European Rotorcraft Forum*, Liverpool, UK, September 2008.

[3] R.J. Jeracki and G.A. Mitchell. Low and high speed propellers for general aviation - performance potential and recent wind tunnel test results. *NASA Techincal Memorandum*, 81745, April 1981.

[4] S. Leth, F. Samuelsson, and S. Meijer. Propeller noise generation and its reduction on the saab 2000 high-speed turboprop. In *4th AIAA/CEAS Aeroacoustics Conference (19th AIAA aeroacoustics conference) Toulouse, France, Paper no 98-2283, pp. 457-463*, June 2-4, 1998.

[5] D.A. McCurdy. Annoyance caused by advanced turboprop aircraft flyover noise. *NASA Technical Memorandum*, 2782, March 1988.

[6] F. R. Menter and Y. Egorov. Sas turbulence modelling of technical flows. *Direct and Large-Eddy Simulation VI*, 10:687–694, 2006.

[7] L. MuÃijller, D. KoÅ¿uloviÄ, and R. Radespiel. Aerodynamic performance of an over-the-wing propeller configuration at increasing mach number. *CEAS Aeronautical Journal*, 5(3):305–317, 2014.

[8] T. Pechan and A. Sescu. Experimental study of noise emitted by propeller's surface imperfections. *Applied Acoustics*, 92:12–17, 2015. cited By 0.

[9] N. Scrase and M. Maina. The evaluation of propeller aero-acoustic design methods by means of scaled-model testing employing pressure tapped blades and spinner. In *Proceedings of the 19th ICAS Congress*, Anheim, CA, USA, 18-23 September 1994.

[10] P.R. Spalart, W-H. Jou, M. Strelets, and S.R. Allmaras. Comments on the Feasibility of LES for Wings, and on a Hybrid RANS/LES Approach. In *Proceedings of the 1st AFOSR International Conference On DNS/LES, Columbus, OH, August 4–8*, 1997.

[11] R. Steijl, G.N. Barakos, and K. Badcock. A framework for CFD analysis of helicopter rotors in hover and forward flight. *International Journal for Numerical Methods in Fluids*, 51:819 – 847, 2006.

[12] C. Wang, L. Zhang, X. Zheng, and S. Wei. Prediction of propeller noise in steady flow based on combining les and i-fem. *Harbin Gongcheng Daxue Xuebao/Journal of Harbin Engineering University*, 36(1):91–97, 2015.

[13] R.P. Woodward and I.J. Loeffler. In-flight source noise of an advanced large-scale single-rotation propeller. *Journal of Aircraft*, 30(6):918–926, Nov-Dec 1993.

[14] S.-Y. Wu and S. Li. Numerical analysis for noise induced by vibration of propeller blades. *Zhendong yu Chongji/Journal of Vibration and Shock*, 33(12):207–210, 2014.